Modeling the Adenosine Receptors: Comparison of the Binding Domains of A_{2A} Agonists and Antagonists

Soo-Kyung Kim,[†] Zhan-Guo Gao,[†] Philippe Van Rompaey,[§] Ariel S. Gross,[†] Aishe Chen,[†] Serge Van Calenbergh,[§] and Kenneth A. Jacobson*[,†]

Molecular Recognition Section, Laboratory of Bioorganic Chemistry, National Institute of Diabetes and Digestive and Kidney Diseases (NIDDK), National Institutes of Health (NIH), Bethesda, Maryland 20892 and Laboratorium voor Medicinale Chemie (FFW), Harelbekestraat 72 B-9000 Gent, Belgium

Received January 27, 2003

A three-dimensional model of the human A_{2A} adenosine receptor (AR) and its docked ligands was built by homology to rhodopsin and validated with site-directed mutagenesis and the synthesis of chemically complementary agonists. Different binding modes of A_{2A}AR antagonists and agonists were compared by using the FlexiDock automated docking procedure, with manual adjustment. Putative binding regions for the 9*H*-purine ring in agonist NECA **3** and the 1*H*-[1,2,4]triazolo[1,5-*c*]quinazoline ring in antagonist CGS15943 **1** overlapped, and the exocyclic amino groups of each were H-bonded to the side chain of $N^{6.55}$. For bound agonist, H-bonds formed between the ribose 3′- and 5′-substituents and the hydrophilic amino acids $T^{3.36}$, $S^{7.42}$, and $H^{7.43}$, and the terminal methyl group of the 5′-uronamide interacted with the hydrophobic side chain of $F^{6.44}$. Formation of the agonist complex destabilized the ground-state structure of the A_{2A}AR, which was stabilized through a network of H-bonding and hydrophobic interactions in the transmembrane helical domain (TM) regions, facilitating a conformational change upon activation. Both flexibility of the ribose moiety, required for the movement of TM6, and its H-bonding to the receptor were important for agonism. Two sets of interhelical H-bonds involved residues conserved among ARs but not in rhodopsin: (1) $E13^{1.39}$ and $H278^{7.43}$ and (2) $D52^{2.50}$, with the highly conserved amino acids $N280^{7.45}$ and $S281^{7.46}$, and $N284^{7.49}$ with $S91^{3.39}$. Most of the amino acid residues lining the putative binding site(s) were conserved among the four AR subtypes. The A_{2A}AR/**3** complex showed a preference for an intermediate conformation about the glycosidic bond, unlike in the A_3AR/**3** complex, which featured an anti-conformation. Hydrophilic amino acids of TMs 3 and 7 (ribose-binding region) were replaced with anionic residues for enhanced binding to amine-derivatized agonists. We identified new neoceptor (T88D)-neoligand pairs that were consistent with the model.

Introduction

The adenosine receptors (ARs), classified as A_1, A_{2A}, A_{2B}, and A_3 subtypes, represent a physiologically and pharmacologically important family of G protein-coupled receptors (GPCRs).[1] ARs are important pharmacological targets in the treatment of a variety of diseases because of their key roles in controlling numerous physiological processes. For example, many therapeutic agents under development for treatment of central nervous system disorders, inflammatory diseases, asthma, kidney failure, and ischemic injuries exert their effects via interactions with ARs.

We are particularly interested in the ligand interactions of the A_{2A}AR because of current interest in its relation to inflammatory conditions and movement disorders[2,3] and because the results of point mutagenesis are known for this subtype.[4−6] A_{2A}AR agonists are also potentially useful for the treatment of cardiovascular diseases, such as hypertension, ischemic cardiomyopathy, inflammation, and atherosclerosis,[7] and A_{2A}AR antagonists have been proposed as novel therapeutics for Parkinson's disease and may also be active as cognition enhancers, neuroprotective and antiallergic agents, analgesics, and positive inotropics.[8−10] Although the physiological effects mediated through the A_{2A}AR have been extensively investigated, only a few molecular modeling studies, which used a low-resolution rhodopsin template,[4,11] have explored the binding properties of agonists and antagonists at the A_{2A}AR. The development of more potent and/or selective A_{2A}AR antagonists and agonists is still being pursued intensively.

Extensive mutagenesis was carried out for both the A_1 and A_{2A} ARs and to a lesser extent for the A_{2B} and A_3 ARs.[1,12] The retinal binding site of rhodopsin,[13] a G protein-coupled photoreceptor, and the putative ligand-binding sites on ARs, as deduced by using mutational analysis, overlap extensively. Most of the essential residues required for recognition of AR agonists and/or antagonists, which bind within the transmembrane helical domains (TMs) 3, 5, 6, and 7,[1] coincide largely with the corresponding amino acids of the binding site of *cis*-retinal in rhodopsin, although there are additional interaction sites within TMs 6 and 7 of the ARs in comparison with the binding site of rhodopsin (Table 1). Recently, the ground-state X-ray structure of rhodopsin with 2.8-Å resolution[13] has advanced our under-

* Corresponding author: Dr. K. A. Jacobson, Chief, Molecular Recognition Section, Bldg. 8A, Rm. B1A-19, NIH, NIDDK, LBC, Bethesda, MD 20892-0810, Tel.: 301-496-9024, Fax: 301-480-8422, E-mail: kajacobs@helix.nih.gov.
[†] National Institutes of Health.
[§] Laboratorium voor Medicinale Chemie.

10.1021/jm0300431 CCC: $25.00
Published on Web 10/10/2003

Table 1. Mutational Analysis for Selected Residues of the ARs with Respect to Ligand Binding

	rhodopsin	A_{2A}[a]	mutational results	A_1[b]	mutational results
TM 1	A42$^{1.37}$	T11		G14	T: increased Ag affinity[55]
	M44$^{1.39}$	**E13**	Q: slight reduction of Ag but not Ant affinity[24]	**E16**	A/Q: Ag affinity reduced 4- to 40-fold; little change in Ant affinity[25]
	P53$^{1.48}$	L22		P25	L: modest reduction of Ag affinity[55]
	L59$^{1.54}$	C28		I31	C: NC in radioligand binding[55]
TM2	Y74$^{2.41}$	Y43		C46	A/S: NC in ligand binding[56]
	N78$^{2.45}$	S47		S50	A: NC in ligand binding[25]
	D83$^{2.50}$	D52		D55	A: increase in Ag affinity with NC in Ant affinity; disrupted regulation of Ag binding by sodium ions[25]
	S93$^{2.60}$	F62		L65	F: NC in radioligand binding[55]
TM3		C77		C80	A/S: no detectable radioligand binding[56]
	L112$^{3.27}$	F79		M82	F: NC in radioligand binding[55]
	E113$^{3.28}$	I80		V83	
	G114$^{3.29}$	A81		A84	
	F115$^{3.30}$	C82		C85	A: NC in radioligand binding, S: Ag affinity reduced 4- to 13-fold; NC in Ant affinity[56]
	F116$^{3.31}$	F83		**P86**	F: substantial reduction of Ag binding[55]
	A117$^{3.32}$	**V84**	A/D: loss of Ag & Ant radioligand binding, L: slight ↑ in Ag (N^6-substituent) & ↓ in Ant affinity[57]	V87	A: NC in ligand affinity[55]
	T118$^{3.33}$	L85		**L88**	A: substantial ↓ of Ag & Ant binding[55]
	G121$^{3.36}$	**T88**	A/S/R/D/E: substantial ↓ in Ag but not Ant activity[6]	**T91**	A: substantial ↓ of Ag & Ant binding[55]
	E122$^{3.37}$	Q89	A: slight ↑ in Ag and Ant activity, D: slight ↑ in Ag but not Ant affinity, N/S/L: marginal changes in ligand binding, H/R: Ant binding affected[6]	**Q92**	A: substantial ↓ of Ag & Ant binding[55] H95A in A_3: substantial ↓ of Ag & Ant binding[12]
	I123$^{3.38}$	S90	A: marginal changes in ligand binding[6]	S93	A: NC in radioligand binding[25]
	A124$^{3.39}$	S91	A: marginal changes in ligand binding[6]	S94	A: no detectable Ag & Ant binding, T: minor changes[25]
EL2		**E151**	A/Q/D: loss of Ag & Ant binding, ~1000-fold ↓ in Ag potency[5]		K152A in A_3: substantial ↑ in Ant binding. NC in Ag binding[12]
	Ser186	A165		K168	
	Cys187	C166		**C169**	A/S: no detectable radioligand binding[56]
	Ile189	F168		F171	
		E169	A: loss of Ag & Ant binding, ~1000-fold ↓ in Ag potency, Q: gain in N^6-substituted Ag affinity[5]	E172	
	Tyr191	D170	K: NC in ligand binding[5]	K173	
		P173	R: NC in ligand binding[5]	S176	
TM5	Y206$^{5.41}$	F180	A: minor changes in ligand binding[4]	F184	
	M207$^{5.42}$	N181	S: modest reduction of Ag binding[4]	N185	
	F208$^{5.43}$	**F182**	A: loss of Ag & Ant binding, Y, W: modest reduction of Ag binding[4]	F186	
	F212$^{5.47}$	V186		V190	
TM6	**F261**$^{6.44}$	F242		F243	
	W265$^{6.48}$	W246		**W247**	W243A,F in A_3: substantial ↓ in Ant, NC in Ag binding, 400-fold ↓ in Ag potency[12]
	Y268$^{6.51}$	L249		L250	
	A269$^{6.52}$	**H250**	A: loss of Ag & Ant binding, *no Ag activity in functional assays*, F, Y: modest reduction of Ag binding; no effect on Ant binding, N: slight ↑ in Ag affinity, minor changes in Ant affinity[4,57]	**H251**	L: Ant affinity reduced 4-fold; NC in Ag affinity (*Bovine A_1 AR*)[58]
	A272$^{6.55}$	**N253**	A: loss of Ag & Ant radioligand binding[4]	**N254**	N250A in A_3: loss of Ag & Ant binding[12]
	F273$^{6.56}$	C254	A: minor changes in ligand binding[4]	C255	A/S: NC in binding[56]
	F276$^{6.59}$	**F257**	A: loss of Ag & Ant radioligand binding[4]	L258	
	H278$^{6.61}$	C259		C260	A/S: NC in binding[56]
		C262	G: NC in radioligand binding[5]	C263	A/S: NC in binding[56]
TM7	**M288**$^{7.35}$	M270		I270	M: canine/bovine A_1 AR binding selectivity[59]
	A292$^{7.39}$	**I274**	A: loss of Ag & Ant binding, 30-fold ↓ in Ag potency[4]	I274	
	F293$^{7.40}$	V275		F265	
	A295$^{7.42}$	**S277**	A: substantial ↓ in only Ag activity and potency, T/C/N/E: marginal changes in binding[4,6]	**T277**	A: substantial ↓ in Ag affinity; NC in Ant affinity, S: modest ↓ in Ag affinity; NC in Ant affinity[59,60,61]
	K296$^{7.43}$	**H278**	A: loss of Ag & Ant binding; 300-fold ↓ in Ag potency, Y: modest reduction of Ag binding; NC on Ant binding, D/E: marginal changes in binding[4,47]	**H278**	L: loss of Ag & Ant binding (*Bovine A_1 AR*)[58] H272E in A_3: substantial ↓ of Ag & Ant binding except N^6-substituted Ag act.[17]
	A299$^{7.46}$	**S281**	A: loss of Ag and Ant radioligand binding; *no Ag activity in functional assay*, T: enhanced activity for Ag, N: marginal changes in ligand binding[4,47]	S281	
		R309		C309	A/S: NC in radioligand binding[56]

Bold entries in the second column indicate residues found to be within the retinal binding site, 5.0 Å. The residues with bold face in ARs were demonstrated important for ligand binding in point-mutation experiments.[1] Ag=agonist; Ant=antagonist; NC= no change. [a] The mutational results of the A_{2A}AR in the present study are included. [b] The mutational results of the A_3AR[12] are included and indicated as A_3. The numbering scheme used here in the superscript is based on the most conserved positions in each helix. Each identifier is composed of a number from 1 to 7 that identifies the helix and, separated by a period, a number associated with a position in that helix. The position number is given relative to the most conserved residue in that helix, which takes the number 50 (N in TM1, D in TM2, R—from DRY—in TM3, W in TM4 and P in TMs 5, 6 and 7).

Chart 1. Structures of the Known A_{2A}AR Agonists and Antagonists Used in Initial Receptor Docking[a]

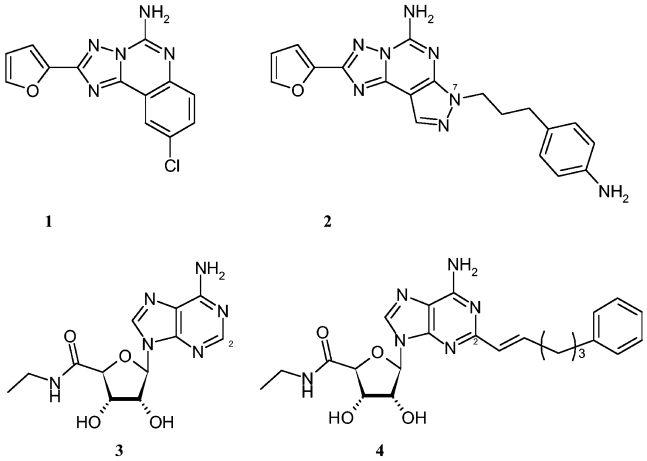

[a] Affinities (K_i: nM) and selectivity ratios are 1, CGS15943, nonselective antagonists; 2, A_{2A}-selective antagonists (hA_{2A}: 0.22, hA_1: 2160, hA_1/hA_{2A}: 9820); 3, nonselective agonist; 4, A_{2A}-selective agonist (rA_{2A}: 3.5, rA_1: 1017, A_1/A_{2A}: 291).[18,24]

standing of the structure and activation of GPCRs. Although the sequence homology between rhodopsin and GPCRs is very low, different amino acids or alternate microdomains can support similar deviations from the regular α-helical structure, thereby resulting in a similar tertiary structure.[14] Thus, it may be possible to extend the binding site and activation models of ARs by using indirect structural data.

In the present study, we constructed a three-dimensional model of the TMs, composed of seven α-helical segments, including portions of the extracellular and cytosolic loops, for the A_{2A}AR, with the high-resolution structure of rhodopsin as a template.[11] In this paper, we describe a comparison of the binding characteristics of A_{2A} agonist and antagonist ligands (Chart 1). In addition, using an A_{2A}-selective antagonist **2** and agonist **4**, we investigated the bound conformations and the basis for selectivity for the human A_{2A}AR. We also made comparisons to our previously published A_3AR model,[15,16] which was derived with similar methods. Finally, the model was tested experimentally by making complementary changes in the structures of agonist ligands (e.g., introduction of amino groups into known ligands, resulting in adenosine derivatives **5**−**8**; Chart 2) and the A_{2A}AR, to form neoceptor−neoligand pairs.[17]

Results and Discussion

Chemical Synthesis. The synthesis of 9-(3-*C*-aminomethyl-3-deoxy-β-D-ribofuranosyl)-N^6-(3-iodobenzyl)-adenine (**7**) is depicted in Scheme 1. The 3-*C*-azidomethyl sugar **9** was prepared in six steps from 1,2-*O*-isopropylidene-D-xylofuranose by reported procedures.[18−20] Removal of the 5-*O*-(*tert*-butyldimethyl)silyl group of **9** with tetrabutylammonium fluoride (TBAF) and protection of the 5-OH group as a toluoyl ester gave **10**. Acidic deblocking of the 1,2-*O*-isopropyl moiety of **10**, followed by acetylation furnished the peracylated 3-*C*-azidomethyl sugar **11**. It should be pointed out that the protecting group exchange was necessary to avoid pyranose ring formation that, in our hands, occurred upon acidic deprotection of **9** (contrary to what was reported[19]). Vorbrüggen-type coupling[21] of **11** with silylated 6-chloropurine[22] gave **12**. Displacement of the chloro atom with 3-iodobenzylamine and deprotection in 7 N NH_3 in MeOH produced the 3′-*C*-azidomethyl nucleoside **13** in an overall yield of 51% (from **11**), improving the N^6-(3-iodobenzyl)adenine coupling previously described.[17] Reduction of the azido moiety with triphenylphosphine gave access to the 3′-*C*-aminomethyl nucleoside **7**.

Chart 2. Structures of the A_{2A}AR Agonists Containing Amino Groups for Electrostatic Interaction with Negatively Charged Side Chains of Mutant A_{2A}ARs[a]

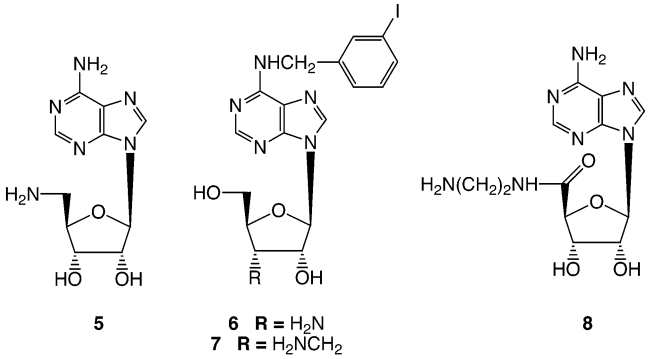

[a] Compounds **5**, **6**, and **8** were used in the previous neoceptor study of the A_3AR.[17]

Scheme 1. Synthetic Route Used To Prepare Compound **7**[a]

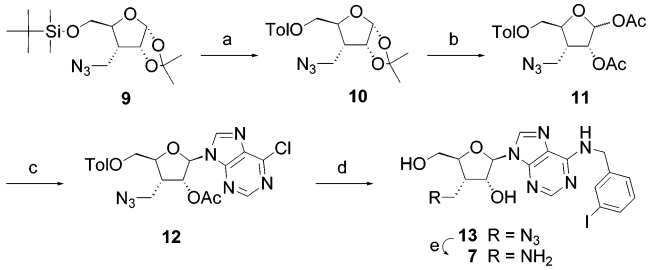

[a] Reagents: (a) (i) TBAF, THF, rt; (ii) toluoyl chloride, pyridine, rt; (b) (i) 50% CH_3COOH, 50 °C (ii) $(CH_3CO)_2O$, pyridine, rt; (c) silylated 6-chloropurine, TMSOTf, dry 1,2-dichloroethane, reflux; (d) (i) 3-iodobenzylamine HCl, Et_3N, EtOH, reflux (ii) 7 N NH_3 in methanol, rt; (e) Ph_3P, NH_4OH, pyridine, rt.

Construction of the A_{2A}AR Molecular Model. As has been done with recent GPCR modeling,[15,23] we have included loop regions, which serve as topological constraints to aid in determining the packing of the attached α-helices within the TM bundle. To decrease the large deviation at the end of the TM bundle, all three-dimensional structures of the A_{2A}AR except the C-terminal region were constructed with the use of homology modeling from the X-ray structure of rhodopsin.[13] To validate the reliability of the model, stereochemical accuracy, packing quality, and folding reliability were checked. A Ramachandran plot was used to compare the ϕ and φ angles with the crystal structure of rhodopsin. All helical amino acids were located in the region of the Ramachandran plot favoring a right-handed α-helix. Only 3.3% of the residues of the loops were in a sterically disallowed region. Calculated ω angles for the A_{2A} model, as in the experimental structure of rhodopsin, indicated the absence of *cis*-peptide bonds. The chirality of all C_α atoms except Cys showed an *S*-configuration. Indicative of the packing quality, there were no bump regions in the calculated

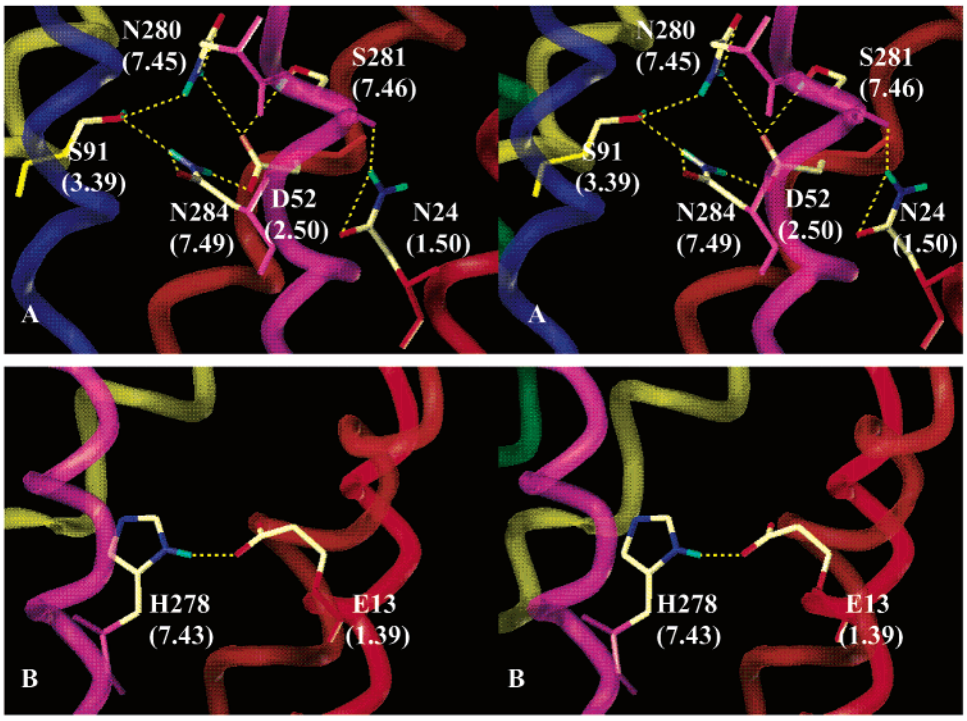

Figure 1. Stereoview showing major interhelical H-bonding networks detected in the unoccupied hA_{2A}AR, between TM1 and TM7 which do not occur in rhodopsin (B) and those involving in addition TM2 and TM3 as found in rhodopsin (A). The H-bonds are represented in yellow.

A_{2A}AR model. Indicative of the folding reliability, the rmsd (root-mean-squared deviation) between backbone atoms in the TMs of the calculated A_{2A}AR and the template molecule was calculated to be 1.27 Å. Both structures, especially the parts with well-defined secondary structures, showed overall similarities.

Conserved H-Bond Networks. The transmembrane region of rhodopsin is stabilized by a number of interhelical H-bonds and hydrophobic interactions, most of which are mediated by highly conserved residues in GPCRs.[13] For example, in the case of the unoccupied A_{2A}AR (Figure 1A), $N24^{1.50}$ interacted with the backbone carbonyl groups of $S281^{7.46}$ and $D52^{2.50}$, as was observed in rhodopsin, which had interhelical H-bonds between the highly conserved $N55^{1.50}$ and the backbone carbonyl groups of $A299^{7.46}$ and $D83^{2.50}$. Another Asn residue, $N78^{2.45}$, in rhodopsin formed H-bonds to $S127^{3.42}$, $T160^{4.49}$, and $W161^{4.50}$. The corresponding amino acid in the A_{2A}AR, $S47^{2.45}$, showed the same hydrophilic interaction with $S94^{3.42}$ and $W129^{4.50}$. With respect to the highly conserved (D/E)R(Y/W) motif in GPCRs, the carboxylate of $E134^{3.49}$ in rhodopsin formed a salt bridge with the guanidium group of the adjacent $R135^{3.50}$, which was also associated with E247 and T251 in TM6. The corresponding amino acids in the A_{2A}AR were D101-R102−Y103. The analogous interactions occurred in the A_{2A}AR, i.e., the salt bridge of $R102^{3.50}$ with $D101^{3.49}$ and E228 in TM6. For the NPXXY motif in the TM7 of GPCRs, the hydroxyl group of $Y306^{7.53}$ was close to $N73^{2.40}$ in rhodopsin, which was also highly conserved among GPCRs. The same result appeared with the calculated A_{2A}AR structure, i.e., the OH group of $Y288^{7.53}$ in the A_{2A}AR was located in proximity to the side chain of $N42.^{2.40}$

Two important interhelical H-bonding interactions for highly conserved sequences took place in ARs but not in rhodopsin (Figure 1B). As previously proposed,[11] there was H-bonding between the side chains of $E13^{1.39}$ and $H278^{7.43}$. Mutational results[24] indicated that $E13^{1.39}$ and the corresponding residue in the A_1AR, $E16^{1.39}$, facilitated agonist binding. Another residue, $D52^{2.50}$ in the A_{2A}AR, was highly stabilized by an H-bonding network among the highly conserved amino acids, $N280^{7.45}$, $S281^{7.46}$, and $N284^{7.49}$, which also formed H-bonds with $S91^{3.39}$. Unlike in rhodopsin, there were additional H-bonds in the ARs for $D52^{2.50}$ interacting with hydrophilic amino acids; whereas in rhodopsin, the amino acids that corresponded to those participating in the H-bond network were all alanine residues except $N284^{7.49}$. The corresponding amino acid, $D55^{2.50}$ in the A_1AR, was responsible for sodium binding.[25]

Hydrophobic Region. Among hydrophobic interactions, the conserved $W246^{6.48}$ was typically surrounded by hydrophobic residues from TMs 3, 6, and 7, as was observed for the human A_3AR[15] and another GPCR, the thyrotropin-releasing hormone receptor.[26] Those hydrophobic amino acids near $W246^{6.48}$ were V84, L85, L87, F242, L243, and P248. The hydrophilic aromatic residues H250 and H278 were also in proximity. The indole ring of $W246^{6.48}$ also formed an H-bond with $N280^{7.45}$, which was stabilized through H-bonding with $D52^{2.50}$. Agonist binding would cause a rotation of the Trp side chain, disrupting these interhelical interactions. Thus, the intramolecular contact network might be destabilized, facilitating the conformational change to activate the A_{2A}AR. The experimental results[15] were consistent with this hypothesis: the $W243A^{6.48}$ mutant A_3AR displayed normal agonist binding but no activity in a functional assay.

Binding of a Known Agonist and Antagonist to Mutant Human A_{2A}ARs. A variety of negatively charged side chains were substituted in the A_{2A}AR at

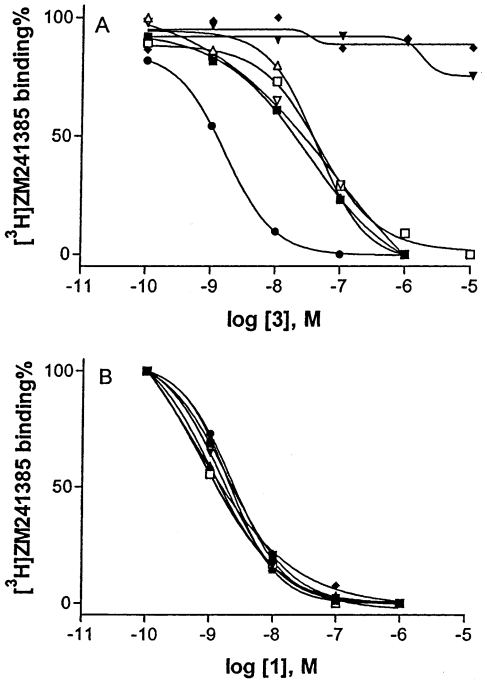

Figure 2. Effect of the agonist NECA **3** and antagonist CGS15943 **1** on the binding of the radiolabeled antagonist [^{3}H]ZM241385 to the human A_{2A}AR. Membranes (10−20 μg of protein) from COS-7 cells transfected with wild type (■) or mutant receptors of T88D (▼), T88E (◆), Q89D (●), S277E (□), H278D (△), or H278E (▽) were incubated with 1.0 nM [^{3}H]ZM241385 in duplicate, together with increasing concentrations of the competing compounds, in a final volume of 0.4 mL of Tris·HCl buffer (50 mM, pH 7.4) at 25 °C for 120 min. Results were from a representative experiment.

Table 2. Binding Affinity of the Nonselective Agonist **3** and Antagonist **1** at WT and Mutant Human A_{2A}ARs[a]

	K_i (nM) or % displacement	
mutant receptor	**3**	**1**
WT	21.4 ± 8.7	0.84 ± 0.22
T88D	20% at 10 μM	0.91 ± 0.09
T88E	0% at 10 μM	0.67 ± 0.17
Q89D	1.5 ± 0.4	0.35 ± 0.12
S277E	29.2 ± 6.3	1.0 ± 0.3
H278D	19.1 ± 3.4	0.41 ± 0.14
H278E	24.6 ± 8.3	0.52 ± 0.06

[a] Membranes from COS-7 cells transfected with WT or mutant A_{2A}AR cDNA were incubated with 1.0 nM [^{3}H]ZM241385 in duplicate, together with increasing concentrations of the competing compounds, in a final volume of 0.4 mL of Tris·HCl buffer (50 mM, pH 7.4) at 25 °C for 120 min. The K_i values are expressed as mean ± standard error from three independent experiments.

hydrophilic positions in TMs 3 and 7 predicted to be in proximity to the bound ribose moiety. Radioligand binding studies showed that T88D and T88E mutant receptors were able to bind the nonselective AR antagonist **1** but not the nonselective AR agonist **3** (Figure 2 and Table 2). Similarly, the T88A mutation was already shown to substantially decrease agonist but not antagonist affinity.[6] For the Q89D mutant receptor, the binding affinity of agonist **3** was increased approximately 14-fold. Its Ala mutation also increased agonist and antagonist binding affinity, but its N/S/L mutation produced only marginal changes in ligand affinity, and its H/R mutation affected only antagonist affinity.[6] However, S277E, H278D, and H278E mutations did not affect the binding of either the agonist **3** or the antagonist **1**. These findings contrasted with the selective decrease of agonist affinity in the S277A mutant receptor and the inability of the H278A mutant receptor to bind either agonist or antagonist radioligand.[4] A total of six mutations—T88D, T88E, Q89D, S277E, H278D, and H278E—did not alter the binding affinity of the antagonist **1**.

Ligand Docking. A crystallographic determination of the human A_{2A} receptor structure would be a better method by which to analyze the conformational implications of our mutagenesis experiments; however, presently no structure is available. While such studies are underway,[27] no structure of close homology to the receptor is available. Thus, we resorted to the widely used, however imprecise, method of rhodopsin-based homology modeling of Family 1 GPCRs. Rhodopsin-based homology modeling is not an automatic method for obtaining a realistic structure for a given GPCR, but rather requires time-consuming custom treatment according to known pharmacological data.[28] In the present study, both agonists and antagonists are docked in the human A_{2A} receptor model. It is to be emphasized that, in general, docking of agonists to GPCR models is subject to even greater uncertainty than antagonist since the template consists of the inactive state of rhodopsin. Often multiple modes of docking of a given agonist or antagonist ligand are observed,[29] and the selection of preference of one docking mode in such cases must be based on diverse pharmacological data, rather than on computational results alone. Nevertheless, the increasing level of refinement of rhodopsin-based homology modeling, for example in the addition of the extracellular loops, has yielded useful insights and results.[30] In the present study, the introduction of complementary functional groups on the ligand and receptor is meant to overcome the problem of ambiguity of docking modes in GPCR modeling.

We used an automated docking procedure (FlexiDock)[31] with manual adjustment to determine the most energetically favorable binding location and orientation for several ligands and compared these results with our previously reported experimental results.[4] An energetically favorable docking mode for each ligand, consistent with the experimental results, was selected from several possible models, which were subjected to a test of consistency with pharmacological results. The most general structural distinction between agonists and antagonists is that only an agonist requires a ribose ring, or more specifically, the 3′- and 5′-ribose substituents that interact directly with the A_{2A}AR.

To explain the different binding properties of antagonists and agonists at the A_{2A}AR, we calculated the conformations of representative ligands, and these structures were docked within the human A_{2A}AR model. The result of FlexiDock showed overlapped binding modes for antagonists and agonists (Figures 3 and 4). Although additional mutational experiments were needed to confirm the reliability of the docked complexes, the result of FlexiDock correlated well with known mutational results.[4] The agonist binding region was similar to our previous A_{2A}AR docking results,[4] which did not consider the flexibility of the ligand.

Antagonist Binding. 5-Amino-9-chloro-2-(2-furyl)-1,2,4-triazolo[1,5-c]quinazoline (CGS15943) **1** is a potent

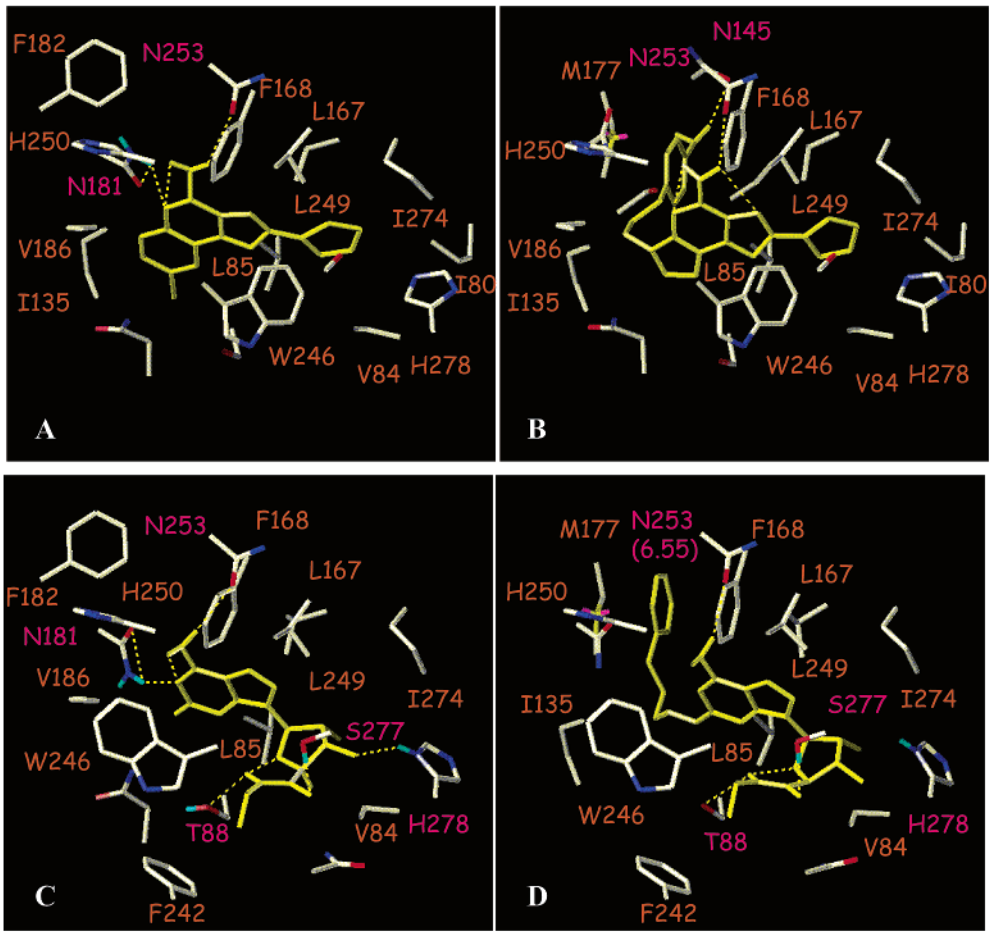

Figure 3. The complex of the A_{2A}AR with agonists and antagonists. (A) CGS15943, a nonselective antagonist; (B) an A_{2A}-selective antagonist; (C) NECA, a nonselective agonist; (D) an A_{2A}-selective agonist. All ligands are represented in yellow. The amino acids of the A_{2A}AR that are depicted in red and orange participated in the hydrophilic and hydrophobic interactions, respectively.

and nonselective adenosine antagonist that we used as a modeling template in previous studies.[32] The major mode of interaction of **1** with the A_{2A}AR consisted of hydrophobic interactions (Figures 3A and 4A). Large hydrophobic pockets consisting mostly of residues at TMs 3, 6, and 7 interacted with the ligand. Hydrophobic amino acids that participated in these interactions with the ligand were L85$^{3.33}$, I135$^{4.56}$, L167 (EL2), F168 (EL2), F182$^{5.43}$, V186$^{5.47}$, W246,$^{6.48}$ and L249$^{6.51}$ near the quinazoline ring and I80$^{3.28}$, V84$^{3.32}$, and I274$^{7.39}$ in proximity to the furan ring. One important hydrophilic interaction was an H-bond formed between the exocyclic amino group at the 5-position and N253$^{6.55}$. Additional weak H-bonding between the side chain of N181$^{5.42}$ and N^6 of the CGS15943 served to increase the thermal stability of the complex. This docking result was consistent with our previously reported Ala mutant receptors—F182A, H250A, N253A, I274A, and H278A—all of which lost the high-affinity binding of both A_{2A}AR agonists and antagonists. The aromatic residue H250 also appeared to be a required component of this mainly hydrophobic pocket. H-Bonding to this residue was not essential, as indicated by retention of function in F and Y mutant receptors.[4]

A series of pyrazolo[4,3-*e*]-1,2,4-triazolo[1,5-*c*]pyrimidine derivatives was developed by Baraldi and coworkers as potent and selective nonxanthine A_{2A} antagonists.[33] The addition of the 4-aminophenylpropyl group at the N^7-position of the triazolopyrimidine ring produced a highly A_{2A}-selective antagonist **2** (K_i = 0.22 nM, hA_1/hA_{2A}= 9820), which did not significantly interact with either A_{2B} or A_3 ARs.[34] Its derived structure—activity relationships indicate that the tricyclic structure of the pyrazolotriazolopyrimidine, the presence of the furan ring, the exocyclic 5-amino group, and the arylalkyl substituent on the nitrogen at the 7-position are probably essential for both affinity and selectivity for the A_{2A}AR subtype. To investigate the structural requirements that increase high affinity and selectivity for the A_{2A}AR, we carried out a docking study of this A_{2A}-selective antagonist **2**. Additional hydrophobic interactions between the 4-aminophenylpropyl moiety and the hydrophobic pocket at TM4 and TM5 and H-bonding of the 4-amino group with N145 (EL2) both could contribute to the increase of A_{2A}AR affinity (Figure 3B). An equilibrium thermodynamic study, which showed a higher binding equilibrium enthalpy value for the pyrazolotriazolopyrimidine derivative containing a hydroxyl group at the para-position of the phenyl ring than for its analogue lacking the hydroxyl group, suggested the presence of an electrostatic interaction (probably an H-bond) involved in recognition of the hydroxyl moiety within the binding site.[35]

The A_{2A}AR sequence alignment indicated that most of the amino acids in the putative binding site within 5Å of the A_{2A}-selective antagonist **2** were conserved among ARs. Highly conserved amino acids were L85$^{3.33}$, T88$^{3.36}$, G136$^{4.57}$, P139$^{4.60}$, F168 (EL2), M177$^{5.38}$, F182$^{5.43}$,

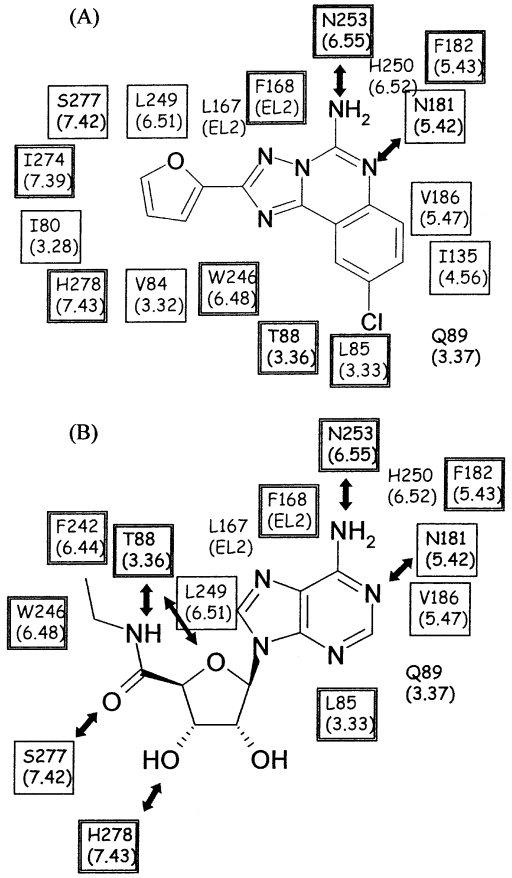

Figure 4. Detailed interactions with **1** (A) and **3** (B) in the putative A_{2A} binding site. The residues in the double-squared box are highly conserved among G protein-coupled receptors, and those in the single-squared box are conserved amino acids among ARs.

W246$^{6.48}$, N253$^{6.55}$, I274$^{7.39}$, and H278$^{7.43}$. However, in the docked complex the amino acids located near the N,^{5} N,^{7} and N^8 positions of the triazolo[1,5-*c*]pyrimidine varied. The proximity of L167 (E for A_1, Q for A_3) and H250$^{6.52}$ (S for A_3) to the ribose 5′-position and Q89$^{3.37}$ (H for A_3) to the adenine 8-position could account for the reported experimental result that the N^5-unsubstituted derivatives showed high affinity for the A_{2A}AR subtype, whereas the *N*^{5}-phenylcarbamoyl and *N*^{8}-methyl substituents at the pyrazolo[4,3-*e*]-1,2,4-triazolo-[1,5-*c*]pyrimidine as the same core molecule increased affinity and selectivity for the A_3AR subtype (K_i = 0.16 nM, hA_1/hA_3 = 3,710, hA_{2A}/hA_3 = 2381, hA_{2B}/hA_3 = 1390):[36] On one hand, hydrophilic amino acids such as Q167 and S247 in the A_3AR near the putative binding region for N^5 substituents would be expected to increase the selectivity for the A_3 subtype through additional H-bonding with carbamoyl groups. On the other hand, the bulky and aromatic side chains such as L167 and H250 in the A_{2A}AR made it easy to accommodate an unsubstituted *N*^{5}-amino group. H95 in the A_3AR near the 8-position binding region had a more hydrophobic character than did the homologous Ser in the A_1, A_{2A}, and A_{2B} ARs, possibly explaining the fact that the hydrophobic factor at the N^8-position was important for A_3AR binding.[37] Residues V186$^{5.47}$ (I for A_3) and I135$^{4.56}$ (V for A_1 and A_3) appeared to contribute to the high affinity at the A_{2A}AR through interaction with N^7-substitutions of the pyrazole ring,[37] such as a propyl group. The size of the side chain at positions 4.56 and 5.47 may be important for an optimal van der Waals interaction, although the hydrophobic character of these two side chains is similar: with a longer side chain at this position, i.e., I$^{5.47}$ in the A_3AR, steric repulsion occurred, and with a shorter size, i.e., V$^{4.56}$ in A_1 and A_3, van der Waals attractive forces were not optimal. Thus, the molecular modeling results were supported by the evidence that N^5-, N^7-, and N^8-substituents of pyrazolotriazolopyrimidine analogues controlled the subtype selectivity of binding to ARs.[38]

Agonist Binding. The environment surrounding the purine ring of A_{2A} agonists binding in our current A_{2A}AR model was very similar to that of the triazolopyrimidine ring of antagonists, including the H-bonding of the exocyclic amino group with the highly conserved N253$^{6.55}$. As we expected from the structural differences between the agonists and antagonists, a characteristic feature of agonist binding was additional H-bond formation of the 3′-OH with H278$^{7.43}$ and of the 5′-amide group of **3** with T88$^{3.36}$ and S277$^{7.42}$ (Figures 3C, 3D, and 4B). However, with our former A_{2A}AR model[4] we reported different hydrophilic interactions: (1) H-bonds between the 5′-OH in adenosine or 5′-NH in **3** and S277$^{7.42}$ and H278$^{7.43}$ and (2) H-bonds between T88$^{3.36}$ and both the 2′-O and 3′-O. In both cases, T88$^{3.36}$ and S277$^{7.42}$ were important only for agonist but not antagonist binding. H278$^{7.43}$ participated in the binding differently, as its hydrophilic interaction with agonists and aromatic interaction with antagonists were the result of the dual role of the imidazole ring. Our present model is consistent with several experimental results concerning recognition of ribose-containing ligands (i.e., adenosine agonists): (1) The hydrophilic interactions at S277$^{7.42}$ and H278$^{7.43}$ were required for high-affinity binding of agonists but not antagonists.[6] The toleration of ligand binding in the S277E and H278D/E mutant receptors suggested that the acidic residues in the mutant receptors retained the ability to form an H-bond with the ligand, i.e., at the 3′-OH group. With respect to the 5′-carbonyl group of **3**, the model suggested that a weak H-bond (2.42 Å and 152.62°), or alternately a water-mediated H-bond, was possible. (2) Radioligand binding studies (Figure 2 and Table 2) showed that T88D and T88E mutant receptors were able to bind the antagonist **1** but not the agonist **3**. Similarly, the T88A mutation was already shown to substantially decrease agonist but not antagonist affinity.[6] Thus the reason that mutation of T88 was specific for diminishing the affinity of the ribosides appeared to be the proximity of this residue to agonists but not antagonists based on the docking result. (3) Replacement of H278 with other aromatic residues was not tolerated in ligand binding.[4]

To better understand the increase of A_{2A} selectivity on substitution of the C^2 of the adenine ring, we performed the docking of the (*E*)-2-phenylpentenyl derivative of NECA **4** (K_i values, nM: rA_{2A}, 3.5; rA_1, 1020; A_1/A_{2A}= 291).[39] Additional hydrophobic interactions between the phenylpentenyl moiety at the 2-position of the adenine ring and the hydrophobic pocket formed from TM4 and TM5 increased the A_{2A}AR affinity, similar to the result shown for the A_{2A}-selective antagonist binding. The interaction sites of the additional phenyl rings were very close to each other. The

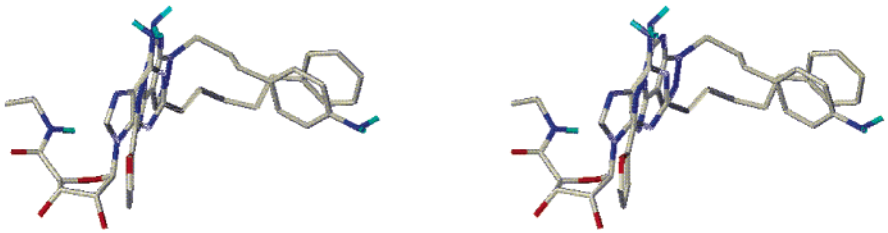

Figure 5. Stereoview showing the superimposition of the bound conformations of the A_{2A}-selective antagonist **2** and agonist **4** in the putative binding sites. The colors represent atom type.

superimposition of the bound conformations of the A_{2A}-selective agonist **4** and antagonist **2** in their putative binding sites demonstrated the partial overlap of the binding sites of the adenine and triazolopyrimidine rings and their C^2 and N^7 substituents (Figure 5). The energies of A_{2A}AR complex formation with **4** and its geometric isomer were calculated. The complex with (*E*)-2-(phenylpentenyl) derivative **4** was more energetically favored than the one with the corresponding (*Z*)-2-(phenylpentenyl) analogue, consistent with experimental results showing that the E-isomers in this series were more potent and selective than were the *Z*-isomers.[38]

The anti-conformation of the glycosidic bond of **3** and other agonists was energetically favorable as an active conformation for A_3AR binding;[15] this was supported by both a molecular modeling study and a binding preference for the methanocarba-ring system in the (*N*)-conformation, which favors the anti-conformation.[40,41] However, the A_{2A}AR complex with its agonist showed a preference for the intermediate conformation about the glycosydic bond. The χ angles (O4′−C1′−N9−C8) of **3** and **4** docked in the A_{2A}AR were −74.4° and −66.2°, respectively. There might be subtle differences in binding requirements, conformational preferences, and local environments among subtypes of ARs, although most of the amino acid sequences in the putative binding sites (TM regions) are conserved among the four types of ARs. The electrostatic potential maps of the A_{2A} and A_3 ARs showed some differences in the shape and electrostatic nature of their binding sites near the second extracellular loop (Figure 6).

Conformational Hypothesis for Activation of the A_{2A}AR. Agonist binding was significantly different than antagonist binding in the region of the ribose ring, as expected from the requirement for a ribose ring in the agonist but not in the antagonist. Thus, the putative ribose-binding region is probably involved in receptor activation. For the A_3AR,[15] we tried to gain insight into the distinct structural requirements for binding and activation by using ligand effects on cyclic AMP production in intact CHO (Chinese hamster ovary) cells and docking a few adenosine analogues. An interesting result concerned the conserved $W243^{6.48}$ side chain in the A_3AR, which was involved in recognition of the classical (nonnucleoside) A_3AR antagonists but not adenosine-derived ligands and which displayed a characteristic movement—counterclockwise rotation as viewed from the exofacial side—exclusively upon docking of agonists.[15] We concluded similarly for the A_{2A}AR that a significant distinction between agonists and antagonists was whether ligand binding could effect the movement of $W246^{6.48}$ side chain (Figure 3). Additional binding of the ribose 5′-substituents shown in the agonist complex induced the movement of the side-chain

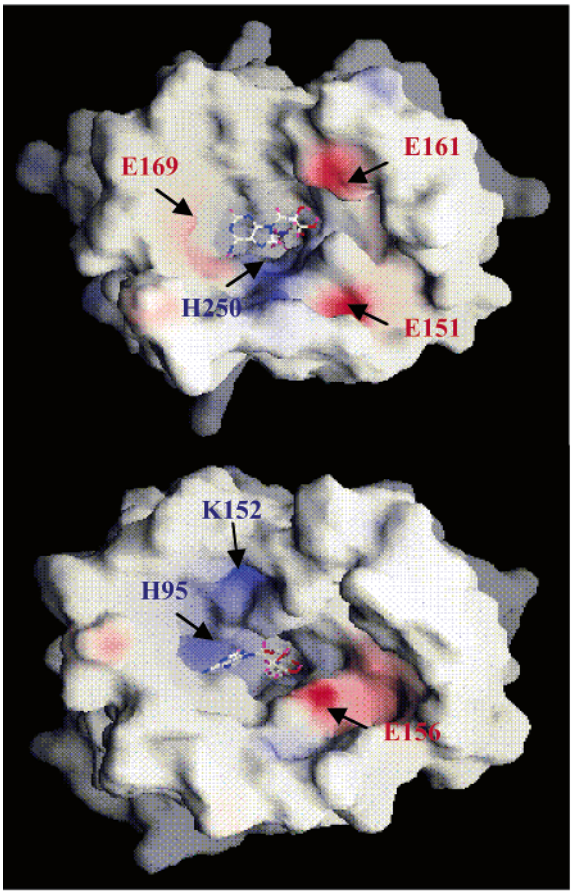

Figure 6. Electrostatic potential map made with the Grasp program. Putative binding sites of the A_{2A}AR (top) and A_3AR (bottom), with the second extracellular loop removed from the extracellular view. NECA **3** is represented as a stick model. Blue and red color potential indicates the electronic positive and negative, respectively.

of $W246^{6.48}$. That conformational change might disrupt a network of H-bonding of $W246^{6.48}$ with $N280^{7.45}$, which participated in the H-bonding network of $D52^{2.50}$, as well as hydrophobic interactions of $W246^{6.48}$ with hydrophobic residues from TMs 3, 6, and 7, thus facilitating a conformational change upon receptor activation. If the A_{2A}AR behaves like the A_3AR,[15] then flexibility of the ribose moiety and specific recognition elements at the 3′- and 5′-positions, to permit the movement of TM6, would be important for agonism at the A_{2A}AR. The modeling result indicated that the overall flexibility and binding elements of the ribose ring were important for distinguishing the receptor interactions of agonists and antagonists. It also correlated with recent studies[42] based on electron paramagnetic resonance and fluorescence spectroscopy, which suggested an outward movement of the cytoplasmic end of TMs 3 and 6, as well as

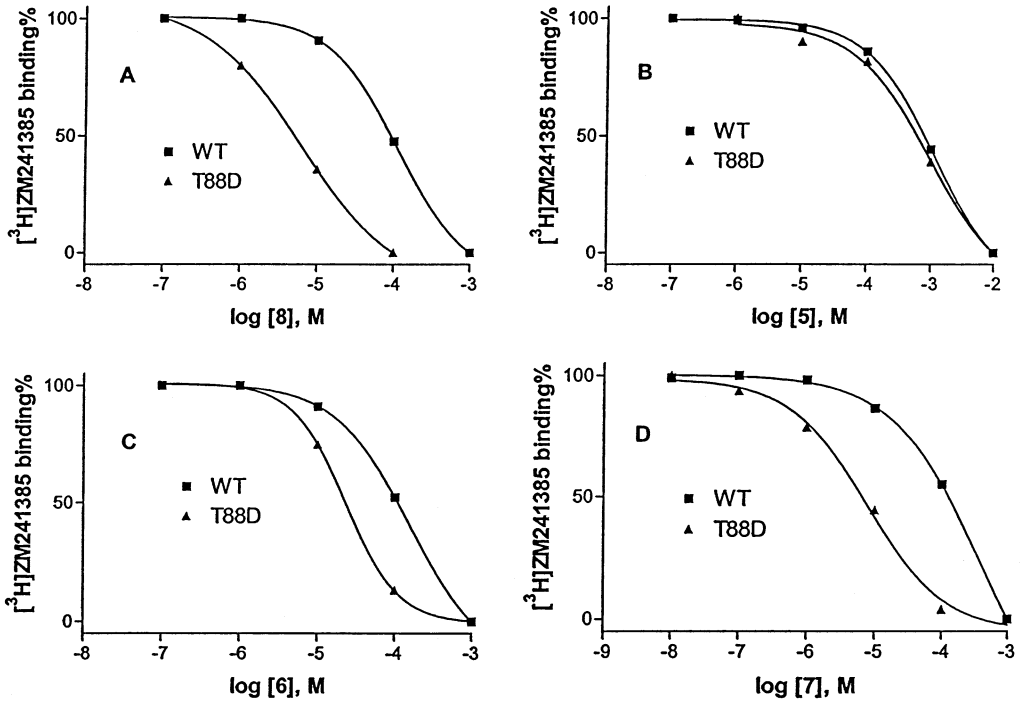

Figure 7. Effect of the amino derivatives of adenosine **8** (A), **5** (B), **6** (C), and **7** (D) on the binding of the radiolabeled antagonist [^{3}H]ZM241385 to the human A_{2A}AR. Membranes (10−20 μg of protein) from COS-7 cells transfected with wild type or T88D mutant receptor. Membranes were incubated with 1.0 nM [^{3}H]ZM241385 in duplicate, together with increasing concentrations of the competing compounds, in a final volume of 0.4 mL of Tris·HCl buffer (50 mM, pH 7.4) at 25 °C for 120 min. Results were from a representative experiment. The K_i values were from three independent experiments and are listed in Table 3.

an anticlockwise rotation of TM6 around its helical axis as viewed from the extracellular side.

Two of the three most conserved prolines in GPCRs, P6.50 and P7.50, occur on TM6 and TM7. P6.50 is in proximity to the binding site, i.e., W246$^{6.48}$. P7.50 was near N284$^{7.49}$, which associated with D52$^{2.50}$, the putative sodium-binding site, through H-bonding. It was proposed that in rhodopsin P6.50 acts as a flexible hinge, straightening TM6 upon light-induced activation.[43] Thus, these two proline residues that are conserved among GPCRs would facilitate the agonist-induced movement of TM6 and subsequently TM7 to rearrange intracellular loop (IL) 3 and helix 8, which are known to be important for the receptor−G protein interface.[44]

Amino Derivatives of Adenosine as Neoligands for Neoceptors Derived from the A_{2A}AR. The current model, like the A_3AR model,[15] suggested the ribose moiety was in proximity to hydrophilic residues of TM3. This hypothesis was tested experimentally by making complementary changes in the structures of the agonist ligand (i.e., introducing a positively charged ammonium group) and the receptor (i.e., introducing a negatively charged carboxylate group) to provide a new electrostatic interaction as the basis of neoceptor−neoligand pairs. Four amino derivatives (Chart 2) were tested in binding to a variety of Asp and Glu mutant receptors (Table 3). The 5′-aminoethyluronamide **8** (equivalent to appending an amino group at the end of the 5′-substituent of **3**) displayed a large selective enhancement in binding to the T88D mutant receptor (Figure 7). Also, compound **7** displayed a significant enhancement of affinity at the same mutant receptor. However, other possible electrostatic interactions of the ribose 3′-amino groups of compounds **6** and **7** with negatively charged mutant receptors, such as H278E, as suggested in the model, were not supported in the binding assay.

Table 3. Binding Affinity of Amino Derivatives of Adenosine (see Chart 2) at WT and Mutant Human A_{2A}ARs[a]

	K_i (μM)			
	5	**6**	**7**	**8**[b]
WT	534 ± 51	67 ± 13	79 ± 16	46.1 ± 4.2
T88D	407 ± 142	18 ± 7	6.5 ± 1.9	4.4 ± 1.6
T88E	492 ± 161	57 ± 8	64 ± 28	57 ± 19
Q89D	52 ± 9	6.4 ± 0.9	58 ± 18	3.6 ± 1.0
S277E	604 ± 125	88 ± 36	67 ± 11	41 ± 8
H278D	−	87 ± 36	59 ± 19	121 ± 32
H278E	−	64 ± 5	56 ± 6	72 ± 14

[a] Membranes from COS-7 cells transfected with WT or mutant A_{2A}AR cDNA were incubated with 1.0 nM [^{3}H]ZM241385 in duplicate, together with increasing concentrations of the competing compounds, in a final volume of 0.4 mL of Tris·HCl buffer (50 mM, pH 7.4) at 25 °C for 120 min. The K_i values are expressed as mean ± standard error from three independent experiments. [b] **8**, MRS3366.

For the docking studies of neoceptor and neoligand,[17] three mutant receptors—T88D, S277D, and H278E—were optimized through a molecular dynamics (MD) procedure after the mutation of each side chain. T88, S277, and H278 residues in the inactive state of A_{2A}AR preferred the gauche+ (g+) rotamer conformation, which also occurred in the bound state of the A_{2A}AR/**3** complex. However, in the T88D mutant receptor, the side chain of aspartate residue was in the trans (t) form, because of new H-bonding of the carboxylate group with N181$^{5.42}$. Thus, there was a local conformational change with respect to the wild type in the position and direction of the aspartate side chain. This conformational change was consistent with the binding profile of the neoceptor. Initially, on the basis of the model of the unoccupied native A_{2A}AR, the 5′-amino derivative

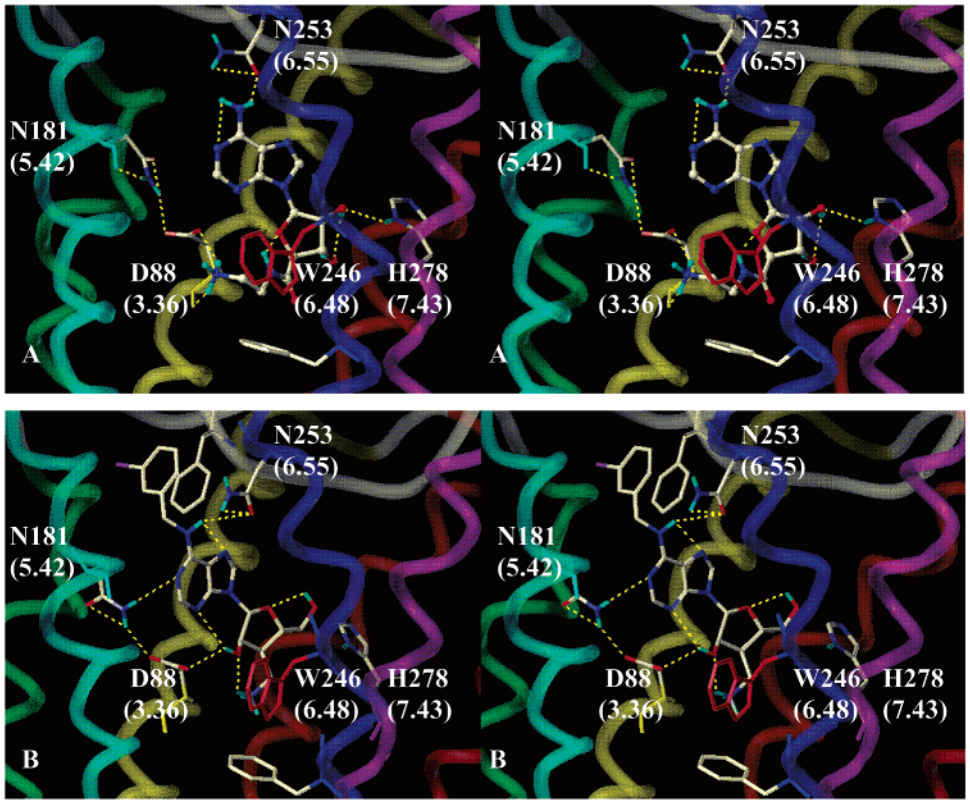

Figure 8. Stereoview showing the complex of the T88D neoceptor with neoligand. (A) Compound **8** with 5′-aminoethyluronamide group. (B) Compound **7** with a 3′-aminomethyl group (represented in the protonated form). The neoligands are represented as ball-and-stick models. The intermolecular H-bonding between neoceptor and neoligand is displayed as yellow color. The W246$^{6.48}$ of the T88D A_{2A}AR in red shows the movement of the indole side chain upon ligand binding.

5 was expected to display an enhanced affinity for the neoceptor T88D. However, **5** did not display an increase of binding affinity, whereas compound **8** with the extended ammonium group was enhanced in affinity. The docking result of compound **8** suggested the possibility of the salt bridge (2.82 Å) and H-bonding (2.03 Å) between acidic residues of D88 and the terminal ammonium ion but the loss of H-bonding at the 3′- and 5′-position, as suggested in **3** binding to the wild-type A_{2A}AR (Figure 8A). Compound **7** was additionally substituted at the N^6-position and also displayed binding enhancement at the T88D mutant receptor. In the docking of **7**, a different binding mode that was energetically unfavorable in the A_{2A}AR/**3** complex was suggested, because with side-chain geometry that was identical to that of the A_{2A}AR/**3** complex, it was impossible for the 3′-ammonium group of **7** to interact with the side chain of D88. In its complex, the conjugation of H-bonding between D88 and 3′-ammonium ion through the 2′-OH group was suggested. An additional interaction of the N^6-benzyl group of **7** with the second extracellular loop, especially through hydrophobic interaction with F168, was evident in the model (Figure 8B); however, there was no interaction of the 5′-OH with this neoceptor. The conformational search of compounds **6** and **7** indicated that the lowest-energy conformer of compound **7** had more stable intramolecular H-bonding of the 2′-OH group and the 3′-ammonium ion (1.86 Å) than was displayed by compound **6** (2.45 Å). It was consistent with the experimental result: i.e., compound **7** showed a greater increase of binding affinity to its neoceptor than compound **6** did. Thus, we identified new neoceptor (T88D)−neoligand pairs consistent with the theoretical model, even though the binding affinities to the T88D neoceptor were still low compared to the endogenous ligand binding to the wild-type A_{2A}AR.

Conclusions

The molecular modeling results clearly delineated the interactions involved in the binding of agonists and antagonists, which correlated well with known experimental results. Flexibility and binding character at the 3′- and 5′-positions of the ribose ring were required for a movement of TM6, which was correlated with receptor activation. The docking complexes provided insight into the conformational and binding requirements for agonists and antagonists at the A_{2A}AR. Structural differences between the A_{2A}AR and the A_3AR include the microenvironment surrounding docked agonist and antagonist ligands and the glycosidic bond angle of docked agonists. Structural similarities between the A_{2A}AR and the A_3AR include H-bond networks involving the putative sodium binding site, a hydrophobic region surrounding W246$^{6.48}$, and the proposed rotation of TM6 to induce receptor activation. The introduction of a hydrophilic moiety such as ribose into an otherwise hydrophobic region destabilizes the inactive ground state of the receptor and thus would facilitate activation. Furthermore, this study is intended to facilitate further design of both adenosine analogues and nonpurines targeted for improved A_{2A}AR affinity and selectivity, including neopceptor−neoligand pairs.[17] The identification of the T88D receptor as a new neoceptor that may be activated selectively by synthetic ligands, such as **7** and **8**, provides a new means to apply the beneficial effects of A_{2A}AR activation.[1−3] Moreover, this putative

electrostatic interaction, which enhances affinity by anchoring the ligand in the agonist binding site, also serves to validate the model. The positively charged neoligands were docked in the neoceptor to suggest an electrostatic explanation for the selectively enhanced affinity.

Experimental Section

Materials. Human A_{2A}AR cDNA (expression vector pSVL-A_{2A}) was kindly provided by Dr. Marlene Jacobson (Merck Research Labs, West Point, PA). Taq polymerase for the polymerase chain reaction was purchased from PerkinElmer (Norwalk, CT). All enzymes used in this study were obtained from New England Biolabs (Boston, MA). Oligonucleotides used were synthesized by Bioserve Biotechnologies (Laurel, MD). [^{3}H]ZM241385 (4-(2-[7-amino-2-(2-furyl)1,2,4]triazolo-[2,3a][1,3,5]triazin-5-ylamino]ethyl)phenol, 17 Ci/mmol) was from Tocris Cookson Ltd. (Bristol, United Kingdom). Adenosine deaminase, CGS15943, and NECA were obtained from Sigma (St. Louis, MO). All other compounds were obtained from standard commercial sources and were of analytical grade.

Site-Directed Mutagenesis. The protocols used were as described in the QuikChange Site-directed Mutagenesis Kit (Stratagene, La Jolla, CA). Mutations were confirmed by DNA sequencing.

Transient Expression of Wild-Type and Mutant Receptors in COS-7 Cells. COS-7 cells were grown in 100-mm cell culture dishes containing Dulbecco's modified Eagle's medium supplemented with 10% fetal bovine serum, 100 units penicillin/mL, 100 μg streptomycin/mL, and 2 μmol glutamine/mL. Cells were washed with phosphate-buffered saline (with calcium) and then transfected with plasmid DNA (10 μg/dish) by the DEAE (diethylaminoethyl)-dextran method[45] for 1 h. The cells were then treated with 100 μM chloroquine for 3 h in culture medium and cultured for an additional 48 h at 37 °C and 5% CO_2.

Membrane Preparation. After 48 h of transfection, COS-7 cells were harvested and homogenized with a Polytron homogenizer. The homogenates were centrifuged at 20 000 g for 20 min, and the resulting pellet was resuspended in the 50 mM Tris·HCl buffer (pH 7.4) and stored at −80 °C in aliquots. The protein concentration was determined by using the method of Bradford.[46]

Radioligand Binding Assay. The procedures of [^{3}H]-ZM241385 binding to wild-type and mutant human A_{2A}ARs was as previously described.[47] Briefly, membranes (10−20 μg of protein) were incubated with 1.0 nM [^{3}H]ZM241385 in duplicate, together with increasing concentrations of the competing compounds, in a final volume of 0.4 mL Tris·HCl buffer (50 mM, pH 7.4) at 25 °C for 120 min. Binding reactions were terminated by filtration through Whatman GF/B glass-fiber filters under reduced pressure with an MT-24 cell harvester (Brandel, Gaithersburg, MD). Filters were washed three times with ice-cold buffer and placed in scintillation vials with 5 mL scintillation fluid, and bound radioactivity was determined by using a liquid scintillation counter.

Statistical Analysis. Binding and functional parameters were estimated with GraphPad Prism software (GraphPad, San Diego, CA). IC_{50} values obtained from competition curves were converted to K_i values by using the Cheng−Prusoff equation.[48] Data were expressed as mean ± standard error.

Molecular Modeling. All calculations were performed on a Silicon Graphics (Mountain View, CA) Octane workstation (300 MHz MIPS R12000 (IP30) processor). All ligand structures were constructed with the use of the Sketch Molecule of SYBYL 6.7.1.[49] A conformational search of antagonists **1** and **2** was performed by grid search of flexible bonds, rotating at 60°, 180°, and −60° for the propyl group at the N^7 position and 0° or 180° for the bond between the furan and quinazoline rings. The low-energy conformers from the grid search were reoptimized, removing all constraints. A random search for agonists **3** and **4** was performed to obtain thermally stable conformations. The options of random search for all rotatable bonds were 3000 iteration, 3-kcal energy cutoffs, and chirality checking. In all cases, MMFF force field[50] and charge were applied with the use of distance-dependent dielectric constants and conjugate gradient method until the gradient reached 0.05 kcal · mol^{-1}·$Å^{-1}$. After clustering the low-energy conformers from the result of the conformational search, the representative ones from all groups were reoptimized by semiempirical molecular orbital calculations with the PM3 method in the MOPAC 6.0 package.[51]

A human A_{2A}AR model was built by using homology modeling from the recently published X-ray structure of bovine rhodopsin,[13] as we previously described.[17] Multiple-sequence alignment data of selected GPCRs were used for the construction of human A_{2A}AR TM domains.[52] For the model of the second extracellular loop, EL2, two beta-sheet domains in rhodopsin were first aligned, including the disulfide bond between Cys77 and Cys166, and then other parts were added or deleted. To construct the N-terminal region and the intra- and extracellular loops, each alignment was manually adjusted to preserve the overall shape of the loop. Acetyl and *N*-methyl groups blocked the N-terminal and C-terminal regions, respectively, to prevent electrostatic interactions. All helices with backbone constraints and loops were separately minimized. After being combined, all structures were reminimized initially with backbone constraints in the secondary structure and then without any constraints. The Amber all-atom force field[53] with fixed dielectric constant of 4.0 was used for all calculations, terminating when the conjugate gradient reached 0.05 kcal·mol^{-1}·$Å^{-1}$.

For the conformational refinement of the A_{2A}AR and their mutant receptors, the optimized structures were then used as the starting point for subsequent 50-ps MD, during which the protein backbone atoms in the secondary structures were constrained as in the previous step. The options of MD at 300 K with a 0.2-ps coupling constant were a time step of 1 fs and a nonbonded update every 25 fs. The lengths of bonds with hydrogen atoms were constrained according to the SHAKE algorithm.[54] The average structure from the last 10-ps trajectory of MD was reminimized with backbone constraints in the secondary structure and then without all constraints as described above.

For the accuracy of the three-dimensional A_{2A}AR model, the distribution of the main chain torsion angles φ and ψ was examined in a Ramachandran plot. Also, all ω angles for the peptide planarity were measured. We checked that all Cα atoms of the receptor backbone amino acid residues were of the L-configuration. The rmsd between backbone atoms in all helices was compared with the X-ray structure of rhodopsin as a template. The coordinates of the optimized human A_{2A}AR model (1upe) are available from the Protein Data Bank at www.rcsb.org/pdb/.

Flexible docking was facilitated through the FlexiDock utility in the Biopolymer module of SYBYL 6.7.1 (Tripos, St. Louis, MO). During flexible docking, only the ligand was defined with rotatable bonds. After the hydrogen atoms were added to the receptor, atomic charges were recalculated by using Kollman All-atom for the protein and Gasteiger-Hückel for the ligand. H-bonding sites were marked for all residues in the active site and for ligands that were able to act as H-bond donor or acceptor. Ligands were variously prepositioned in the putative binding cavity guided by point mutation results as a starting point for FlexiDock. Default FlexiDock parameters were set at 3000-generation for genetic algorithms. To increase the binding interaction, the torsion angles of the side chains that directly interacted within 5 Å of the ligands, according to the results of FlexiDock, were manually adjusted. Finally, the complex structure was minimized by using an Amber force field with a fixed dielectric constant (4.0), until the conjugate gradient reached 0.1 kcal·mol^{-1}·$Å^{-1}$.

Acknowledgment. We thank Dr. Marlene Jacobson (Merck, West Point, PA) for the gift of the plasmid coding the human A_{2A}AR. We thank Dr. Gary Stiles (Duke University, Durham, NC) for the gift of CHO cells

expressing the human A_3AR, and Dr. Joel Linden (University of Virginia, Charlottesville, VA) for the gift of CHO cells expressing the human A_1AR and A_{2A}ARs. S.-K.K. and Z.-G.G. thank Gilead Sciences (Foster City, CA) for financial support. We thank Dr. Neli Melman for technical assistance.

Supporting Information Available: Synthetic methods for preparation of compound **7**. This material is available free of charge via the Internet at http://pubs.acs.org.

References

(1) Fredholm, B. B.; IJzerman, A. P.; Jacobson, K. A.; Klotz, K.-N.; Linden, J. International Union of Pharmacology. XXV. Nomenclature and Classification of Adenosine Receptors. *Pharmacol. Rev.* **2001**, *53*, 527−552.

(2) Cassada, D. C.; Tribble, C. G.; Long, S. M.; Kaza, A. K.; Linden, J.; Rieger, J. M.; Rosin, D.; Kron, I. L.; Kern, J. A. Adenosine A_{2A} agonist reduces Paralysis after Spinal Cord Ischemia: Correlation with A_{2A} Receptor Expression on Motor Neurons. *Ann. Thorac. Surg.* **2002**, *74*, 846−849.

(3) Ohta, A.; Sitkovsky, M. Role of G-Protein-Coupled Adenosine Receptors in Downregulation of Inflammation and Protection from Tissue Damage. *Nature* **2001**, *414*, 916−920.

(4) Kim, J.; Wess, J.; van Rhee, A. M.; Schöneberg, T.; Jacobson, K. A. Site-directed Mutagenesis Identifies Residues Involved in Ligand Recognition in the Human A_{2a} Adenosine Receptor. *J. Biol. Chem.* **1995**, *270*, 13987−13997.

(5) Kim, J.; Jiang, Q.; Glashofer, M.; Yehle, S.; Wess, J.; Jacobson, K. A. Glutamate Residues in the Second Extracellular Loop of the Human A_{2a} Adenosine Receptor Are Required for Ligand Recognition. *Mol. Pharmacol.* **1996**, *49*, 683−691.

(6) Jiang, Q.; van Rhee, M.; Kim. J.; Yehle, S.; Wess, J.; Jacobson, K. A. Hydrophilic Side Chains in the Third and Seventh Transmembrane Helical Domains of Human A_{2A} Adenosine Receptors Are Required for Ligand Recognition. *Mol. Pharmacol.* **1996**, *50*, 512−521.

(7) Stone, T. W.; Collis, M. G.; Williams, M.; Miller, L. P.; Karasawa, A.; Hillaire-Buys, D. Adenosine: Some Therapeutic Applications and Prospects. In *Pharmacological Sciences: Perspectives for Research and Therapy in the Late 1990s*; Cuello, A. C., Collier, B., Eds.; Birkhauser Verlag: Basel, Switzerland, 1995; pp 303−309.

(8) Richardson, P. J.; Kase, H.; Jenner, P. G. Adenosine A_{2A} Receptor Antagonists as New Agents for the Treatment of Parkinson's Disease. *Trends Pharmacol. Sci.* **1997**, *18*, 338−344.

(9) Ledent, C.; Vaugeois, J. M.; Schiffmann, S. N.; Pedrazzini, T.; El Yacoubi, M.; Vanderhaeghen, J. J.; Costentin, J.; Heath, J. K.; Vassart, G.; Parmentier, M. Aggressiveness, Hypoalgesia and High Blood Pressure in Mice Lacking the Adenosine A_{2A} Receptor. *Nature (London)* **1997**, *388*, 674−678.

(10) Baraldi, P. G.; Cacciari, B.; Spalluto, G.; Borioni, A.; Viziano, M.; Dionisotti, S.; Ongini, E. Current Developments of A_{2A} Adenosine Receptor Antagonists. *Curr. Med. Chem.* **1995**, *2*, 707−722.

(11) IJzerman, A. P.; van der Wenden, E. M.; van Galen, P. J. M.; Jacobson, K. A. Molecular Modeling of Adenosine Receptors. II. The Ligand Binding Site on the Rat A_{2a} Receptor. *Eur. J. Pharmacol.: Mol. Pharmacol.* **1994**, *268*, 95−104.

(12) Gao, Z.-G.; Chen, A.; Barak, D.; Kim, S.-K.; Müller, C. E.; Jacobson, K. A. Identification by Site-directed Mutagenesis of Residues Involved in Ligand Recognition and Activation of the Human A_3 Adenosine Receptor. *J. Biol. Chem.* **2002**, *277*, 19056−19063.

(13) Palczewski, K.; Kumasaka, T.; Hori, T.; Behnke, C. A.; Motoshima, H.; Fox, B. A.; Le Trong, I.; Teller, D. C.; Okada, T.; Stenkamp, T. E.; Yamamoto, M.; Miyano, M. Crystal Structure of Rhodopsin: A G Protein-Coupled Receptor. *Science* **2000**, *289*, 739−745.

(14) Ballesteros, J. A.; Shi, L.; Javitch, J. A. Structural Mimicry in G Protein-Coupled Receptors: Implications of the High-Resolution Structure of Rhodopsin for Structure−Function Analysis of Rhodopsin-Like Receptors. *Mol. Pharmacol.* **2001**, *60*, 1−19.

(15) Gao, Z.-G.; Kim, S.-K.; Biadatti, T.; Chen, Q.; Lee, K.; Barak, D.; Kim, S. G.; Johnson, C. R.; Jacobson K. A. Structural Determinants of A_3 Adenosine Receptor Activation: Nucleoside Ligands at the Agonist/Antagonist Boundary. *J. Med. Chem.* **2002**, *45*, 4471−4484.

(16) Our most recent model of the human A_3AR (by Dr. Soo-Kyung Kim) is now available on the pdb ftp site. Entry in PDB format (compressed): pdblo74.ent. Z.; Entry in mmCIF format (compressed): lo74.cif. Z. See *http://www.rcsb.org/pdb/latest_news.html#models_removal2*.

(17) Jacobson, K. A.; Gao, Z. G.; Chen, A.; Barak, D.; Kim, S. A.; Lee, K.; Link, A.; van Rompaey, P.; van Calenbergh, S.; Liang, B. T. Neoceptor Concept Based on Molecular Complementarity in GPCRs: A Mutant Adenosine A_3 Receptor with Selectively Enhanced Affinity for Amine-Modified Nucleosides. *J. Med. Chem.* **2001**, *44*, 4125−4136.

(18) Parr, I. B.; Horenstein, B. A. New Electronic Analogues of the Sialyl Cation: N−Functionalized 4-Acetamido-2,4-dihydroxypiperidines. Inhibition of Bacterial Sialidases. *J. Org. Chem.* **1997**, *62*, 7489−7494.

(19) Lin, T.-S.; Zhu, J.-L.; Dutschman, G. E.; Cheng, Y.-C.; Prusoff, W. H. Syntheses and Biological Evaluations of 3′-Deoxy-3′-*C*-Branched-Chain-Substituted Nucleosides. *J. Med. Chem.* **1993**, *36*, 353−362.

(20) Filichev, V. V.; Brandt, M.; Pedersen, E. B. Synthesis of an Aza Analogue of the 2-Deoxy-d-ribofuranose and Its Homologues. *Carbohydr. Res.* **2001**, *333*, 115−122.

(21) Vorbrüggen, H.; Krolikiewicz, K.; Bennua, B. Nucleoside Synthesis with Trimethylsilyl Triflate and Perchlorate as Catalysts. *Chem. Ber.* **1981**, *114*, 1234−1255.

(22) van Tilburg, E. W.; van der Klein, P. A. M.; von Frijtag Drabbe Künzel, J.; de Groote, M.; Stannek, C.; Lorenzen, A.; IJzerman, A. P. 5′-O−Alkyl Ethers of N, 2-Substituted Adenosine Derivatives: Partial Agonists for the Adenosine A_1 and A_3 Receptors. *J. Med. Chem.* **2001**, *44*, 2966−2975.

(23) Kontoyianni, M.; DeWeese, C.; Penzotti, J. E.; Lybrand, T. P. Three-Dimensional Models for Agonist and Antagonist Complexes with β_2-Adrenergic Receptor. *J. Med. Chem.* **1996**, *39*, 4406−4420.

(24) IJzerman, A. P.; Von Frijtag Drabbe Künzel, J. K.; Kim, J.; Jiang, Q.; Jacobson, K. A. Site-Directed Mutagenesis of the Human Adenosine A_{2A} Receptor. Critical Involvement of Glu^{13} in Agonist Recognition. *Eur. J. Pharmacol.* **1996**, *310*, 269−272.

(25) Barbhaiya, H.; McClain, R.; IJzerman, A.; Rivkees, S. A. Site-Directed Mutagenesis of the Human A_1 Adenosine Receptor: Influences of Acidic and Hydroxy Residues in the First Four Transmembrane Domains on Ligand Binding. *Mol. Pharmacol.* **1996**, *50*, 1635−1642.

(26) Colson, A.-O.; Perlman, J. H.; Jinsi-Parimoo, A.; Nussenzveig, D. R.; Osman, R.; Gershengorn, M. C. A hydrophobic cluster between transmembrane helices 5 and 6 constrains the thyrotropin-releasing hormone receptor in an inactive conformation. *Mol. Pharmacol.* **1998**, *54*, 968−978.

(27) Weiss, H. M.; Grisshammer, R. Purification and characterization of the human adenosine A_{2A} receptor functionally expressed in *Escherichia coli*. *Eur. J. Biochem.* **2002**, *269*, 82−92.

(28) Archer, E.; Maigret, B.; Escrieut, C.; Pradayrol, L.; Fourmy, D. Rhodopsin crystal: new template yielding realistic models of G-protein-coupled receptors? *Trends Pharm. Sci.* **2003**, *24*, 36−40.

(29) Chambers, J. J.; Nichols, D. E. A homology-based model of the human 5-HT_{2A} receptor derived from an *in silico* activated G-protein coupled receptor. *J. Comput. Aided Mol. Des.* **2002**, *16*, 511−520.

(30) Filipek, S.; Teller, D. C.; Palczewski, K.; Stenkamp, R. The crystallographic model of rhodopsin and its use in studies of other G protein-coupled receptors. *Annu. Rev. Biophys. Biomol. Struct.* **2003**, in press.

(31) Judson, R. Genetic Algorithms and Their Use in Chemistry. In *Reviews in Computational Chemistry*, Vol. 10; Lipkowitz, K. B., Boyd, D. B., Eds.; VCH Publishers: New York. 1997; pp 1−73.

(32) Moro, S.; Li, A.-H.; Jacobson, K. A. Molecular Modeling Studies of Human A_3 Adenosine Antagonists: Structural Homology and Receptor Docking. *J. Chem. Inform. Comput. Sci.* **1998**, *38*, 1239−1248.

(33) Baraldi, P. G.; Cacciari, B.; Spalluto, G. P.; de las Infantas y Villatoro, M. J. P.; Zocci, C.; Dionisotti, S.; Ongini, E. Pyrazolo-[4,3-*e*]-1,2,4-triazolo[1,5-*c*]pyrimidine Derivatives: Potent and Selective A_{2A} Adenosine Antagonists. *J. Med. Chem.* **1996**, *39*, 1164−1171.

(34) Baraldi, P. G.; Cacciari, B.; Romagnoli, R.; Spalluto, G.; Monopoli, A.; Ongini, E.; Varani, K.; Borea, P. A. 7-Substituted 5-Amino-2-(2-furyl)pyrazolo[4,3-*e*]-1,2,4-triazolo[1,5-*c*]pyrimidines as A_{2A} Adenosine Receptor Antagonists: A Study on the Importance of Modifications at the Side Chain on the Activity and Solubility. *J. Med. Chem.* **2002**, *45*, 115−126.

(35) Baraldi, P. G.; Cacciari, B.; Spalluto, G.; Bergonzoni, M.; Dionisotti, S.; Ongini, E.; Varani, K.; Borea, P. A. Design, Synthesis, and Biological Evaluation of a Second Generation of Pyrazolo[4,3-*e*]-1,2,4-triazolo[1,5-*c*]pyrimidines as Potent and Selective A_{2A} Adenosine Receptor Antagonists. *J. Med. Chem.* **1998**, *41*, 2126−2133.

(36) Baraldi, P. G.; Cacciari, B.; Moro, S.; Spalluto, G.; Pastorin, G.; Ros, T. D.; Klotz, K.-N.; Varani, K.; Gessi, S.; Borea, P. A. Synthesis, Biological Activity, and Molecular Modeling Investigation of New Pyrazolo[4,3-*e*]-1,2,4-triazolo[1,5-*c*]pyrimidine Derivatives as Human A_3 Adenosine Receptor Antagonists. *J. Med. Chem.* **2002**, *45*, 770−780.

(37) Baraldi, P. G.; Cacciari, B.; Romangnoli, R.; Spalluto, G.; Moro, S.; Klotz, K.-N.; Leung, E.; Varani, K.; Gessi, S.; Merighi, S.; Borea, P. A. Pyrazolo[4,3-*e*]-1,2,4-triazolo[1,5-*c*]pyrimidine Derivatives as Highly Potent and Selective Human A_3 Adenosine Receptor Antagonists: Influence of the Chain at the N^8 Pyrazole Nitrogen. *J. Med. Chem.* **2000**, *43*, 4768−4780.

(38) Baraldi, P. G.; Cacciari, B.; Romangnoli, R.; Spalluto, G.; Klotz, K.-N.; Leung, E.; Varani, K.; Gessi, S.; Merighi, S.; Borea, P. A. Pyrazolo[4,3-*e*]-1,2,4-triazolo[1,5-*c*]-pyrimidine Derivatives as Highly Potent and Selective Human A_3 Adenosine Receptor Antagonists. *J. Med. Chem.* **1999**, *42*, 4473−4478.

(39) Vittori, S.; Camaioni, E.; Francesco, E. D.; Volpini, R.; Monopoli, A.; Dionisotti, S.; Ongini, E.; Cristalli, G. 2-Alkenyl and 2-Alky Derivatives of Adenosine and Adenosine-5′-*N*-Ethyluronamide: Different Affinity and Selectivity of E- and Z-Diastereomers at A_{2A} Adenosine Receptors. *J. Med. Chem.* **1996**, *39*, 4211−4217.

(40) Lee, K.; Ravi, R. G.; Ji, X−d.; Marquez, V. E.; Jacobson, K. A. Ring-Constrained (N)Methanocarba-Nucleosides as Adenosine Receptor Agonists: Independent 5′-Uronamide and 2′-Deoxy Modifications. *Bioorg. Med. Chem. Lett.* **2001**, *11*, 1333−1337.

(41) Jacobson, K. A.; Ji, Xi-*d*.; Li, A.-H.; Melman, N.; Siddiqui, M. A.; Shin, K.-J.; Marquez, V. E.; Ravi, R. G. Methanocarba Analogues of Purine Nucleosides as Potent and Selective Adenosine Receptor Agonists. *J. Med. Chem.* **2000**, *43*, 2196−2203.

(42) Farrens, D. L.; Altenbach, C.; Yang, K.; Hubell, W. L.; Khorana, H. G. Requirements of rigid-body motion of transmembrane helices for light activation of rhodopsin. *Science* **1996**, *274*, 768−770.

(43) Shi, L.; Liapakis, G.; Xu, R.; Guarneri, F.; Ballesteros, J. A.; Javitch, J. A. *β*-Adrenergic Receptor Activation: Modulation of the Proline Kink in Transmembrane 6 by a Rotamer Toggle Switch. *J. Biol. Chem.* **2002**, *277*, 40989−40996.

(44) Liu, J.; Conklin, B. R.; Blin, N.; Yun, J.; Wess, J. Identification of a Receptor/G-Protein Contact Site Critical for Signaling Specificity and G-Protein Activation. *Proc. Natl. Acad. Sci. U.S.A.* **1995**, *92*, 11642−11646.

(45) Cullen, B. R. Use of Eukaryotic Expression Technology in the Functional Analysis of Cloned Genes. *Methods Enzymol.* **1987**, *152*, 684−704.

(46) Bradford, M. M. A Rapid and Sensitive Method for the Quantitation of Microgram Quantities of Protein Utilizing the Principle of Protein-Dye Binding. *Anal. Biochem.* **1976**, *72*, 248−254.

(47) Gao, Z.-G.; Jiang, Q.; Jacobson, K. A.; IJzerman, A. P. Site-Directed Mutagenesis Studies of Human A_{2A} Adenosine Receptors. Involvement of Glu^{13} and His^{278} in Ligand Binding and Sodium Modulation. *Biochem. Pharmacol.* **2000**, *60*, 661−668.

(48) Cheng, Y.-C.; Prusoff, W. H. Relationship between the Inhibition Constant (K_i) and the Concentration of Inhibitor Which Causes 50 Percent Inhibition (I_{50}) of an Enzymatic Reaction. *Biochem. Pharmacol.* **1973**, *22*, 3099−3108.

(49) Sybyl Molecular Modeling System, version 6.7.1. Tripos Inc., St. Louis, MO.

(50) Halgren, T. A. MMFF VII. Characterization of MMFF94, MMFF94s, and Other Widely Available Force Fields for Conformational Energies and for Intermolecular-Interaction Energies and Geometries. *J. Comput. Chem.* **1999**, *20*, 730−748.

(51) Stewart, J. J. P. MOPAC: A Semiempirical Molecular Orbital Program. *J. Comput. Aided Mol. Des.* **1990**, *4*, 1−105.

(52) van Rhee, A. M.; Jacobson, K. A. Molecular Architecture of G Protein-Coupled Receptors. *Drug Devel. Res.* **1996**, *37*, 1−38.

(53) Cornell, W. D.; Cieplak, P.; Bayly, C. I.; Gould, I. R.; Merz, Jr., K. M.; Ferguson, D. M.; Spellmeyer, D. C.; Fox, T.; Caldwell, J. W.; Kollman, P. A. A Second Generation Force Field for the Simulation of Proteins, Nucleic Acids and Organic Molecules. *J. Am. Chem. Soc.* **1995**, *117*, 5179−5197.

(54) Ryckaert, J. P.; Ciccotti, G.; Berendsen, H. J. C. Numerical Integration of the Cartesian Equations of Motion for a System with Constraints: Molecular Dynamics of *n*-alkanes. *J. Comput. Phys.* **1977**, *23*, 327−333.

(55) Rivkees, S. A.; Barbhaiya, H.; IJzerman A. P. Identification of the adenine binding site of the human A_1 adenosine receptor. *J. Biol. Chem.* **1999**, *274*, 3617−3621.

(56) Scholl, D. J.; Wells, J. N. Serine and alanine mutagenesis of the nine native cysteine residues of the human A_1 adenosine receptor. *Biochem. Pharmacol.* **2000**, *60*, 1647−1654.

(57) Jiang Z.; Lee, B. X.; Glashofer, M.; van Rhee, A. M.; Jacobson, K. A. Mutagenesis reveals structure−function parallels between human A_{2A}-adenosine receptors and the biogenic amine family. *J. Med. Chem.* **1997**, *40*, 2588−2595.

(58) Olah, M. E.; Ren H.; Ostrowski, J.; Jacobson, K. A.; Stiles, G. L. Cloning, expression, and characterization of the unique bovine A_1 adenosine receptor. Studies on the ligand binding site by site-directed mutagenesis. *J. Biol. Chem.* **1992**, *267*, 10764−10770.

(59) Tucker, A. L.; Robeva, A. S.; Taylor, H. E.; Holeton, D.; Bockner, M.; Lynch, K. R.; Linden, J. A_1 adenosine receptors. Two amino acids are responsible for species differences in ligand recognition. *J. Biol. Chem.* **1994**, *269*, 27900−27906.

(60) Townsend-Nicholson, A.; Schofield, P. R. A threonine residue in the seventh transmembrane domain of the human A_1 adenosine receptor mediates specific agonist binding. *J. Biol. Chem.* **1994**, *269*, 2373−2376.

(61) Dalpiaz, A.; Townsend-Nicholson, A.; Beukers, M. W.; Schofield, P. R.; IJzerman, A. P. Thermodynamics of full agonist, partial agonist, and antagonist binding to wild-type and mutant adenosine A_1 receptors. *Biochem. Pharmacol.* **1998**, 56, 1437−1445.

JM0300431